

The secondary Bjerknes force on a spherical bubble cluster in a periodic pressure field

周期的に変動する圧力場において球形クラスター気泡にはたららく第二ビヤクネス力

(1 blank line)

Naohiro Sugita^{1†} and Toshihiko Sugiura² (¹Grad. School of Science and Technology, Keio Univ.; ²Department of Mechanical Eng., Keio Univ.)

杉田直広^{1†}, 杉浦壽彦² (¹慶大院理工, ²慶大機械工)

(2 blank lines)

1. Introduction

The cluster bubble dynamics is of particular interest for ultrasound applications because the bubbles in a cluster present complex collective behavior due to strong nonlinear interactions.¹

Although the radial dynamics of a cluster has been addressed for many years², global dynamics such as deformation and translational motion of a cluster bubble is still challenging. In most theoretical works, the configuration of the cluster is assumed to be spherical symmetry, and coalescence and fission³ of the bubbles in the cluster are neglected. However, when the cluster is driven by a strong sound field, the violent collapse leads to breakup of the cluster, and many fission fragments are produced. (some bubbles coalesce again during the next expansion phase). This gives rise to difficulties in experimental treatments and analysing observed phenomena. Thus, understanding the translational dynamics of a bubble cluster gives a greater insight to the macroscopic behavior of a bubbly flow.

In the present study, the translational motion of a spherical bubble cluster in a vibrating water vessel is recorded by a high-speed camera, and the secondary Bjerknes force⁴ acting on the bubble cluster is discussed on the basis of the classical theory.

2. Materials and Methods

2.1 Vibrating vessel

A rectangular acrylic vessel (size: 50×50×150 mm, thickness: 10 mm) with tap water at the room temperature is fixed on and driven by a vibration generator (EMIC, 513-BS/Z08). The height of the water column is 140 mm. A vacuum pump is connected to the vessel through a valve in order to reduce the hydrostatic pressure in the vessel to near that of vapor pressure. This allows large oscillation amplitude to be developed at low driving amplitude.⁵ The driving acceleration generates an

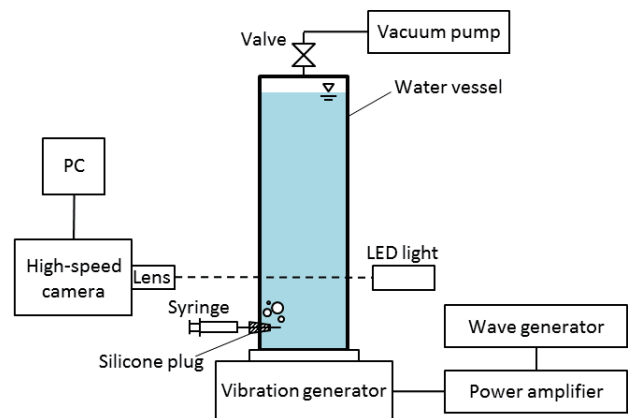


Fig. 1 Schematic of the experimental setup.

uniform pressure gradient in the liquid column so that the pressure distribution in the liquid follows⁶

$$P(y, t) = P_0 + \rho_l \omega^2 A y \sin \omega t \quad (1)$$

where P_0 is the hydrostatic pressure in the vessel, ρ_l is the liquid density, ω and A are the driving angular frequency and amplitude and y is the vertical coordinate measured from the free surface.

The recording system consists of a high-speed video camera (Baumer, HXC20), low magnification zoom lens (KEYENCE, VH-Z00R) and LED light (KEYENCE, CA-DSR3). The recorded rate of the high-speed camera is set to 90 frames/sec.

2.2 Generation of a bubble cluster

Before the vibration driving starts, a millimeter-sized cavitation nucleus is injected from the silicone plug using a needle at the bottom of the vessel. The average nuclei radius is approximately 2 mm for all the observations. The nucleus responds to the pressure change, and the resulting inertial cavitation bubble evolves to a spherical cluster bubble.

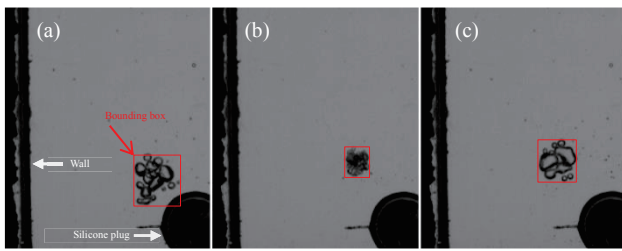


Fig. 2 Volume oscillation of a cluster bubble captured by the high-speed video camera. The recorded rate is 90frames/sec, and the photographs show every fourth frames. The red square is the bounding box which encloses the cluster bubble with the minimum area.

3. Results and Discussion

Volume oscillation of a typical cluster bubble observed is shown in Fig. 2. The cluster departs from the silicone plug [Fig. 2 (a)] and violently collapses [Fig. 2 (b)], producing a number of fission fragments, which coalesce again during the next expansion phase [Fig. 2 (c)]. The driving frequency $\omega/2\pi$ is 190 Hz, and the driving amplitude measured by a laser displacement meter is about 100 μm . Therefore, the maximum pressure amplitude calculated using Eq. (1) is 19.9 kPa at the bottom of the vessel, and the maximum cluster radius is about 3 mm.

The recorded images are analyzed in MATLAB (R2014b, The Mathworks Inc.), and the area and centroid of the of the bounding box (See Fig.1) are obtained. The translation velocity of the centroid is calculated by a simple central difference of the centroid.

Fig. 3 illustrates the trajectory of the cluster bubble. The cluster bubble is attracted to the left wall due to the secondary Bjerknes force between the cluster and its image cluster. As the separation

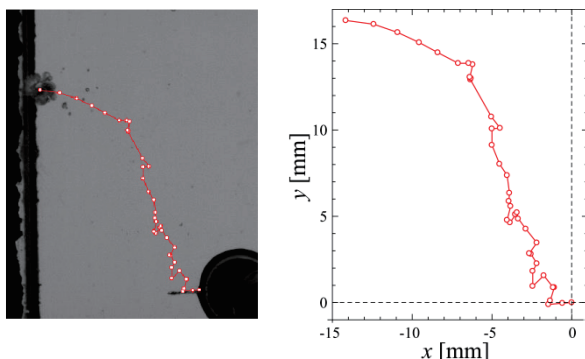


Fig. 3 The trajectory of the cluster bubble. The origin is the initial position of the cluster. The cluster bubble approaches to the left wall (at $x=-15$ mm) due to the Secondary Bjerknes force between the image bubble.

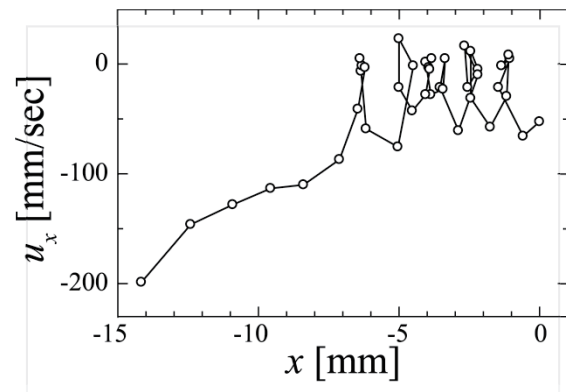


Fig. 4 The horizontal velocity of the cluster centroid as a function of x . The cluster bubble approaches to the left wall (at $x=-15$ mm) due to the Secondary Bjerknes force between the image bubble.

distance decreased, the cluster rapidly accelerates. The horizontal velocity u_x as a function of the bubble horizontal position is described in Fig. 4. It should be noted that the cluster oscillates around the initial position when the separation distance is smaller than 7 mm. However, the velocity suddenly begins to increase with decreasing the separation distance, and the maximum velocity 200 mm/sec is encountered just before the collision to the wall.

Due to coalescence/fission process of the bubbles in the cluster, amplitude of the volume oscillation is randomly changed, and the translational motion becomes highly disorder.

4. Conclusion

The volumetric oscillation and translational motion of a spherical bubble cluster is recorded by a high speed camera. Exceptionally large amplitude oscillation of the cluster bubble is developed in the water vessel with even small amplitude driving. The attractive secondary Bjerknes force between the cluster bubble and its image cluster is observed.

Acknowledgment

This work was supported by Keio University Doctorate Student Grant-in-Aid Program 2015.

References

1. Y. Tanimura, K. Yoshida and Y. Watanabe: Jpn. J. Appl. Phys. **49** (2010) 07HE20-1.
2. E. S. Nasibullaeva and I. S. Akhatov: J. Acoust. Soc. Am. **133** (2013) 3727.
3. C. E. Brennen : J. Fluid Mech. **472** (2002) 153.
4. K. Yoshida, T. Fujikawa and Y. Watanabe : J. Acoust. Soc. Am. **130** (2011) 135.
5. L. A. Crum : J. Acoust. Soc. Am. **57** (1975) 1363.
6. W. L. Nyborg : Biotechnology and Bioengineering **9** (1967) 235.